AD-A060 956 ARMY MISSILE RESEARCH AND DEVELOP..ENT COMMAND REDSTO--ETC F/G 17/7
REAL TIME CORRELATION FOR MISSILE TERMINAL GUIDANCE.(U)
JAN 78 J UPATNIEKS, B D GUENTHER

UNCLASSIFIED DRDMI-H-78-5

NL

END
DATE FILMED
-79
DDC

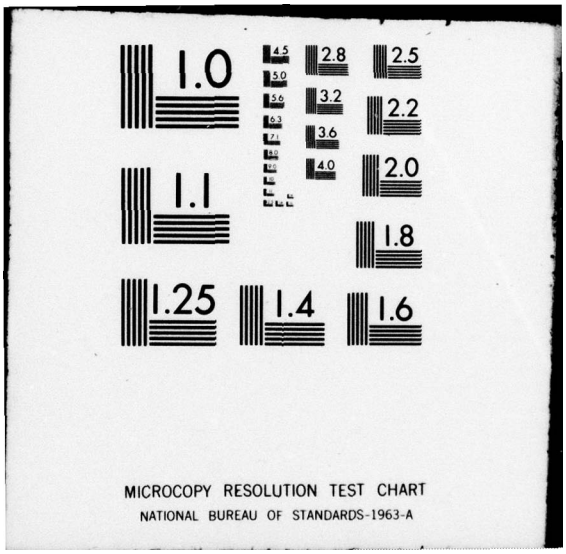
1.0
1.1
1.25
1.4
1.6
1.8
2.0
2.2
2.5
2.8
3.2
3.6
4.0
4.5
5.0
5.6
6.3
7.1
MICROCOPY RESOLUTION TEST CHART
NATIONAL BUREAU OF STANDARDS-1963-A

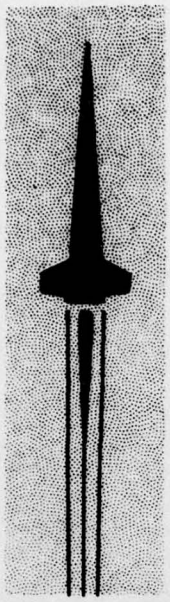



# LEVEL II

TECHNICAL REPORT H-78-5

# REAL-TIME CORRELATION FOR MISSILE TERMINAL GUIDANCE

U.S. ARMY MISSILE RESEARCH AND DEVELOPMENT COMMAND

J. Upatnieks, B. D. Guenther, C. R. Christensen
Missile Research Directorate
High Energy Laser Laboratory

Redstone Arsenal, Alabama 35809

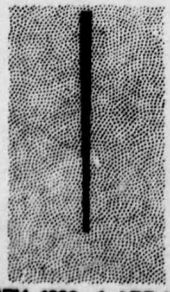

1 January 1978



Approved for Public Release;
Distribution Unlimited.

DMI FORM 1000, 1 APR 77

**DISPOSITION INSTRUCTIONS**

DESTROY THIS REPORT WHEN IT IS NO LONGER NEEDED. DO NOT RETURN IT TO THE ORIGINATOR.

**DISCLAIMER**

THE FINDINGS IN THIS REPORT ARE NOT TO BE CONSTRUED AS AN OFFICIAL DEPARTMENT OF THE ARMY POSITION UNLESS SO DESIGNATED BY OTHER AUTHORIZED DOCUMENTS.

**TRADE NAMES**

USE OF TRADE NAMES OR MANUFACTURERS IN THIS REPORT DOES NOT CONSTITUTE AN OFFICIAL INDORSEMENT OR APPROVAL OF THE USE OF SUCH COMMERCIAL HARDWARE OR SOFTWARE.

UNCLASSIFIED

SECURITY CLASSIFICATION OF THIS PAGE (When Data Entered)

(14) DRDMI-

## REPORT DOCUMENTATION PAGE

READ INSTRUCTIONS BEFORE COMPLETING FORM

| 1. REPORT NUMBER | 2. GOVT ACCESSION NO. | 3. RECIPIENT'S CATALOG NUMBER |
|---|---|---|
| H-78-5 | | |

(6) 4. TITLE (and Subtitle)

REAL TIME OPTICAL CORRELATION FOR MISSILE TERMINAL GUIDANCE.

(9) 5. TYPE OF REPORT & PERIOD COVERED

TECHNICAL REPORT

6. PERFORMING ORG. REPORT NUMBER

(10) 7. AUTHOR(s)

Juris Upatnieks, B. D. Guenther
C. R. Christensen

8. CONTRACT OR GRANT NUMBER(s)

711802-6A-00-7140

9. PERFORMING ORGANIZATION NAME AND ADDRESS

Commander
US Army Missile Research and Development Command
HEL and Research Laboratory
ATTN: DRDMI-HR Redstone Arsenal, Ala 35809

10. PROGRAM ELEMENT, PROJECT, TASK AREA & WORK UNIT NUMBERS

(11)

11. CONTROLLING OFFICE NAME AND ADDRESS

Commander
US Army Missile Research and Development Command
ATTN: DRDMI-TI
Redstone Arsenal, Alabama 35809

12. REPORT DATE

1 Jan 1978

13. NUMBER OF PAGES

41

14. MONITORING AGENCY NAME & ADDRESS (if different from Controlling Office)

(12) 43p.

15. SECURITY CLASS. (of this report)

UNCLASSIFIED

15a. DECLASSIFICATION/DOWNGRADING SCHEDULE

16. DISTRIBUTION STATEMENT (of this Report)

Approved for Public Release; Distribution Unlimited.

17. DISTRIBUTION STATEMENT (of the abstract entered in Block 20, if different from Report)

18. SUPPLEMENTARY NOTES

19. KEY WORDS (Continue on reverse side if necessary and identify by block number)

OPTICAL CORRELATION
MISSILE TERMINAL GUIDANCE
REAL TIME
TERMINAL

20. ABSTRACT (Continue on reverse side if necessary and identify by block number)

A study was conducted to determine the feasibility of using coherent optical correlators for missile terminal guidance. A laboratory area correlator was built which can perform target recognition and location at TV frame rates. This correlator uses an optically addressed liquid crystal image-forming light modulator as an input and holographic matched filters as references. Correlations were performed with optical imagery and simulated radar imagery using a TV monitor to address the modulator. Good cross-correlation signal-to-noise ratios were obtained and the input image could be tracked over a wide →(over)

DD FORM 1 JAN 73 1473 EDITION OF 1 NOV 65 IS OBSOLETE

410 127

UNCLASSIFIED

SECURITY CLASSIFICATION OF THIS PAGE (When Data Entered)

displacement range. Data from these experiments were used to design a compact correlator for typical low resolution radar imagery. The low information content of this imagery allows an array of laser diode sources to be used. By using a corresponding array of matched filter references, up to 900 correlations/second can be performed on 128 x 128 element input imagery and a range of scale, angular orientation, or aspect angle can be searched.

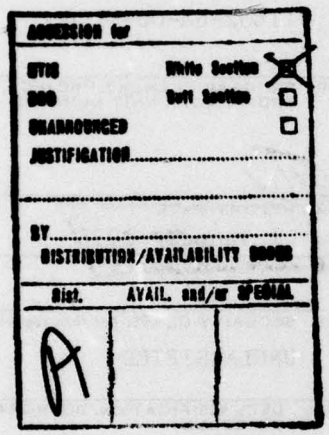

## SUMMARY

Coherent optical correlators are well known to give distinct auto-correlation and cross-correlation peaks between data having precise scale, orientation, and contrast match. These peaks are generally quite narrow and have a low background level because correlations are performed on the high-frequency content of the input image, such as edges and other details. Correlation time is independent of the number of data points on the reference filter and the input image, although in practice the time required to obtain a correlation is determined by the data read-in time and the correlation read-out time.

Experiments were performed with an existing optical correlator to determine typical correlator operating parameters. Special emphasis was placed on correlation of low resolution images because these would be typical for terminal guidance situations. Distinct correlations were obtained with simulated radar images, and data on alignment accuracy of the optical system were obtained.

An optical correlator suitable for guidance applications was designed and its correlation time estimated. The reference filter was assumed to contain 256 × 256 pixels; the input data had 128 × 128 pixels. It was estimated that 50 msec. is required to complete one read-in and erase cycle, and that during this time up to 5 sequential correlations and up to 9 parallel correlations can be performed and read out. The filter library could store up to 225 different reference functions; in addition, scale can be changed by rewriting input data on the input light modulator at different scales.

This proposed optical correlator would have very low power demands. The power consumption of the optical correlator itself, including laser diode light sources and photodiode detector arrays, would be less than 2 W. Additional power would also be required for electronic circuitry to handle data input and output, and to control the operation of the correlator.

The optical correlator can be packaged into 1500 $cm^3$ (0.05 $ft^3$) of space and is expected to weigh less than 5 kg. (12 lb). Additional size and weight reductions could be achieved by miniaturization of components and the use of holographic optical components in place of lenses.

Comparison of optical and digital correlators is somewhat difficult as the limitations of each are in different areas. In terms of its capability to correlate many data points, correlator power consumption, size and correlation speed, the optical correlator is by far the best. Because it is an analog

device, the performance of the optical correlator depends upon the maintenance of component alignment. Alignment should not be a problem in a properly constructed correlator.

For a digital correlator, the major concerns are time and component requirements to take the Fourier transform of the input data and to perform correlations with the reference data. Once the data are digitized, virtually error-free performance can be expected with accuracy limited only by theoretical limitations set by the number of input data points. While this appears to favor a digital approach, the accuracy of the correlator is of questionable value with analog input data. Scale and orientation searches are difficult and time consuming with the digital correlator but are relatively simple and fast with optical correlators.

A brass-board correlator was designed with presently available components. This correlator can be made small and lightweight, with a capability of storing up to 100 reference filters. A variety of tests could be performed with this correlator to demonstrate the feasibility of compact coherent optical correlators.

This study has shown that coherent optical correlators can be smaller and faster than digital correlators and require less power to operate. Excellent correlations with low resolution images of the type used in terminal guidance can be obtained with optical correlators. It is recommended that development of coherent optical correlators be continued with the first step in this development being the construction of a small brass-board correlator as described in this report.

# TABLE OF CONTENTS


| Section | | Page |
|---|---|---|
| 1. | Introduction | 5 |
| 2. | The Experimental System | 8 |
| 3. | Cross-Correlation Experiments | 9 |
| 4. | Experiments with Radar Imagery | 19 |
| 5. | Proposed Correlator Configuration and Performance Estimates | 26 |
| | A. Image and Filter Format | 26 |
| | B. Filter Multiplexing | 27 |
| | C. Estimate of Correlation Time | 28 |
| 6. | Brass-board Correlator | 34 |
| | References | 37 |

# 1. INTRODUCTION

The use of area correlation in terminal guidance requires that the system cross correlate a stored reference with the observed scene and have the capacity for handling variations in aspect angle, rotation, scale and intensity. This correlation must be made in real time at a low false alarm rate.

Digital techniques can accomplish the preceding requirements but have several limiting characteristics. The number of resolution elements that can be processed is limited by the available core memory. Even with well chosen algorithms, a large number of multiplications and additions are required and these increase with the number of resolution elements. For the hypothetical situation of cross-correlation of a reference pattern having 100 × 100 resolution elements against a scene with 200 × 200 elements, $10^4$ multiplications and additions are required for each possible location of the patterns. Because there are $10^4$ possible locations with 100% overlap, $10^8$ operations are required to perform a complete cross-correlation; scale and orientation compensations increase this number further. Parallel processing can reduce the time required to perform this very large number of operations but requires increased complexity and cost.

A recent study has been performed to establish the hardware requirements for using a digital correlation technique. It was concluded in this study that approximately 500 integrated circuits requiring 350 W of power is required to cross-correlate two 128 × 128 pixel pictures using 16 bit arithmetic precision. It was also assumed that eight reference maps would be carried in the processor. Six correlations could be performed on the 128 × 128 reference and 128 × 128 input scene in 0.5 sec. It was assumed that some parallel processing was used to obtain this speed [1].

Optical techniques can be used to perform cross-correlation and have the following advantages. An optical processor has an inherently large information capacity. A relatively modest optical system can handle scenes having over $10^7$ resolution elements. Such a system handles two-dimensional data in a parallel and isotropic manner with a response time dictated by the time required for data input and output. An increase in the number of required resolution elements, for example, through multiplexing, does not increase the response time or size of the optical system. An increase in the complexity of the signal processing is not necessarily accompanied by an increase in cost and complexity of the optical processor.

Optical data processing techniques can be divided into two general categories, incoherent and coherent.

Incoherent optical processing operates on the intensity of the images to be correlated, that is, it handles only positive functions. Coherent processing makes use of both the phase and amplitude of the images and can therefore handle complex functions. A study has been performed that compares the two optical processing techniques [2]. This study demonstrated that typically a much larger output signal-to-noise ratio and greater precision can be obtained using coherent rather than incoherent processing.

Optical processing is only one of several analog techniques that can be used to perform correlation. A comparison of these analog techniques with digital processing has been made [3] and the results show that optical processors now outperform digital systems in speed and cost.

In all correlation systems, variations in the input scene when compared to the on-board reference scene can cause a reduction or loss of the correlation signal. The ability of a processor to handle variations in the input scene will determine if a particular correlation technique is successful. The most common scene deviations are:

### A. Scale

Variations in scale can be reduced by providing the missile with accurate range information. A typical processor can handle errors of ±5% in scale. Larger errors can be handled by one or more of the following techniques:

(1) Additional reference images.

(2) Change in magnification of the imput image digitally by an increase in the size of the matrix or optically through the use of a zoom lens or an electronic variation of the imput transducer.

### B. Rotational Orientation

Variation in rotational orientation can be reduced by providing an attitude control to the missile. A typical optical processor can handle errors of ±2° in rotation. This is a severe error for a digital system and can greatly increase the processing time. To handle this error, the following techniques can be applied:

(1) Additional reference images.

(2) In an optical processor, a dove prism can be mechanically rotated or the image in the input transducer can be electronically rotated.

(3) In a digital processor, the matrix representing the input scene can be rotated.

### C. Intensity

A change of intensity or shading can be a serious problem for a noncoherent processor or a digital processor that matches scenes in real space by an

overlay process or by identification of key features. It is not a problem for those systems that first obtain the Fourier transform of the scene (such as a coherent processor) for they can bandpass filter the spatial frequencies of the scene before correlation.

### D. Aspect Angle

A small change in aspect angle is a distortion of the scene and can be handled by a non-uniform magnification change across the scene area. Large aspect angle changes can create a new scene. For example, a building that was not visible at one aspect angle can become visible at a new aspect angle. This type of variation can only be handled by storing additional reference scenes on-board.

### E. Overlap

A reduction in the signal-to-noise ratio of the correlation can result if the input scene contains information not contained in the reference scene. In the most severe case the input image does not contain any part of the reference image. This problem can be handled by making the reference scene larger than the input scene.

It should be remembered when considering all of these errors that, because of energy requirements, the missile should not be designed to correct to a predetermined trajectory but should be designed to home on the target from a point on the actual trajectory.

In the design of optical processors very little attention is paid to the number of resolution elements in the input because this parameter does not affect the speed of the correlations. However, in the design of digital systems the reduction of this parameter is a major consideration. Thus, the digital and optical systems which have been designed are not equivalent devices and cannot be directly compared.

A sensor on board a missile will typically provide a low resolution scene for the terminal guidance system. A previous study [4] has demonstrated that the use of low resolution imagery reduces the sensitivity of the system to scale and rotation errors in the input scene while still providing an adequate correlation (signal-to-noise ratio greater than 15 dB). Additional advantages are also obtained by the use of low resolution imagery. The size of the optical elements required in the processor is reduced and the coherence requirements on the light source used in the coherent optical processor are reduced, allowing the utilization of laser diodes.

In this report the design of a real time coherent optical processor will be described that will operate using realistic, low resolution input imagery. The design incorporates a bank of

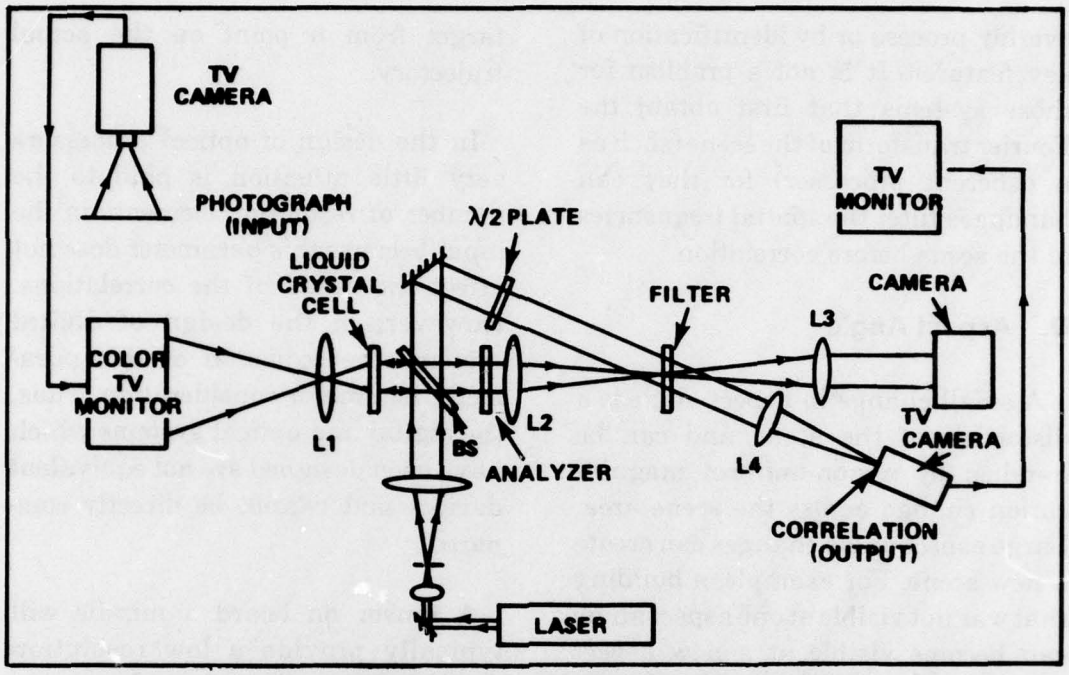


**Figure 1. Schematic of coherent optical correlator.**

reference images to provide the capacity for handling variations in aspect, rotation, and scale. This bank is scanned in time so that it can be determined which reference images are providing correlation signals.

## 2. THE EXPERIMENTAL SYSTEM

Figure 1 shows a schematic of the optical correlator used in laboratory experiments.

A standard TV camera is used to convert a photograph into an electronic signal which is then displayed as a black and white image on a standard color TV monitor. This type of monitor was chosen for its high screen luminescence and good image quality. The image displayed by the monitor was imaged with a 50 mm camera lens, L1, on a liquid crystal incoherent-to-coherent image converter produced by Hughes Aircraft Corporation [5]. The operating area of the converter was a 25 mm square. Laser light incident on this cell had its polarization rotated in proportion to the incoherent scene irradiance, and the coherent image is visible after passing through an analyzer. Lens L2 takes the Fourier transform of the coherent image and displays it at the back focal plane of the lens. A matched filter (the reference) also recorded with this system is located at the Fourier transform plane. The matched filtering operation is performed and the correlation spot displayed either on the face of another standard TV camera or on a film for

recording. A He-Ne laser operating at 6328A° was used and the matched filter recorded on Agfa 10E75 glass plates. Lenses L2 and L4 are 78 mm diameter, 381 mm focal length telescope objectives. The camera is used to photograph the image from the liquid crystal modulator or the image reconstructed from the matched filter. The correlation spot on the TV camera is displayed on the monitor and video lines can be displayed on an oscilloscope and photographed.

A TV monitor input to the correlator was chosen to increase the versatility of the system. The monitor can receive an image from the TV camera, a video tape recorder or a digital processor.

Digital tapes of microwave and far infrared images are available and techniques to enhance the quality of these images are under investigation in this laboratory. The digital processor is interfaced to an active imaging system operating at submillimeter wavelengths. The correlator can, therefore, operate using a large variety of preprocessed or unmodified signals including visible, IR, radar, and submillimeter images.

The correlator can also be operated by imaging an object illuminated with bright artificial light directly on the modulator [6] or by imaging a sunlit outdoor scene or object. A clear weather terminal guidance system with the target or target area imaged directly on the modulator would have a number of advantages including simplicity, light weight, low cost, and high accuracy. However, an all-weather capability, using radar or infrared images, is expected to be required in an operational system and the experimental work reported here is limited to indirect input to the modulator.

## 3. CROSS-CORRELATION EXPERIMENTS

A series of experiments was performed using aerial photographs to demonstrate an area correlation terminal guidance application. Three classes of scenes were chosen which are representative of potential military targets. Photographs made in 1962 were used to record matched filters and these were cross-correlated with photographs of the same areas made in 1970. No attempt was made to optimize the filter parameters for each input image although a K-ratio was chosen to record spatial frequencies between approximately 0.5 *l*/mm and 4 *l*/mm. This yielded good correlation signal-to-noise ratios for all input images.

Figure 2(A) is a photograph of an urban scene on the correlator input monitor. Residential areas can be seen on the left side of the scene and industrial and commercial areas are shown on the right side as they appeared in 1962. Figure 2(B) is the output from the liquid crystal modulator. The total width of the scene imaged on the 25 mm square modulator

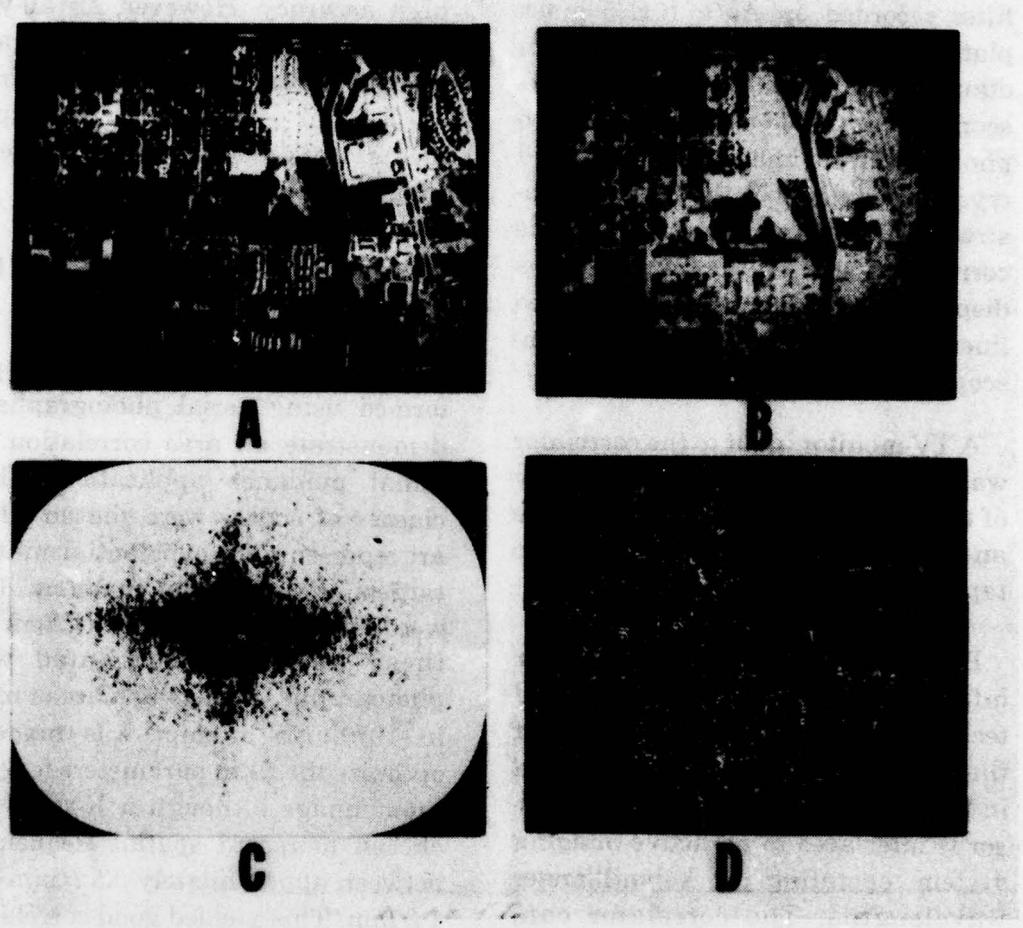


**Figure 2. Urban scene. (a) TV image of urban scene in 1962, (b) modulator output, (c) matched filter made from this scene, and (d) image reconstruction from filter.**

is 1250 m. The matched filter made from this input is shown in Figure 2(C). The 0-50 scale corresponds to 1 mm. A range of spatial frequencies from 0.4 to 5.0 *l*/mm was recorded. Saturation of the emulsion makes the filter opaque near the center, blocking frequencies below 0.4 *l*/mm. The matched filter was illuminated with the reference beam to reconstruct the image in Figure 2 (D). The features on which the filter will correlate are readily seen. The band pass filtering property of the matched filter is apparent from the

edge enhancement in the reconstructed image; therefore, correlations will be obtained on the edges of features in the scene.

A 1970 aerial photograph of the same scene was correlated with the filter made from the 1962 photograph. Cross-correlation and tracking are demonstrated in Figure 3. Figure 3(D) is a triple exposure showing the correlation spot for each of the three positions of the TV input image. The displacement from Figure 3 (A) to Figure 3 (C) corresponds to 425 m on the ground. An oscilloscope trace of a horizontal TV camera scan line though the center correlation spot is shown in Figure 3 (E). Figures 3(D) and 3 (E) are to the same scale. The total length of the scan line is 12.7 mm. The half width at half height for the correlation peak represents approximately 7 m displacement in the scene.

Figure 4 shows a rural scene in 1962 and the matched filter made from it. The high information content of the scene is shown by the density of the filter at high spatial frequencies. this high spatial frequency content is primarily in the woodlands and other vegetation. The image reconstructed from the filter, Figure 4(C), shows the large amount of information recorded on the filter. This produces a very strong auto-correlation and a strong cross-correlation with other images of this scene made at the same time as Figure 4 (A). However, changes in the vegetation may produce a much weaker cross-correlation between images of a rural scene made at different seasons or in different years. This is illustrated in Figure 5 , which shows cross-correlations between a 1970 image and the matched filter in Figure 4(C). Comparison of Figure 4(A) with the aerial photograph in Figure 5 shows that a number of changes in field boundaries, fence rows, and woodlands occured during the eight-year period separating the two photographs. The signal-to-noise ratic in the trace through the correlation spot, Figure 5(E), is therefore somewhat lower than for the urban scene in Figure 3(E). The noise in these traces is electronic noise from the TV camera and the optical signal-to-noise ratio is greater than that shown.

A 1962 view of an airport and the matched filter made from it are shown in Figure 6. Cross-correlation and tracking on a 1970 view of this scene is demonstrated in Figure 7. At this time the airport had been abandoned and residential areas developed at the bottom of the scene.

A scene containing a highway bridge and the matched filter made from this scene are shown in Figure 8. The piers for a second parallel bridge under construction are visible. Cross-correlation with a 1970 photograph of this scene is shown in Figure 9. The scene from which the matched filter was made contained only one bridge. Correlations were obtained on both the

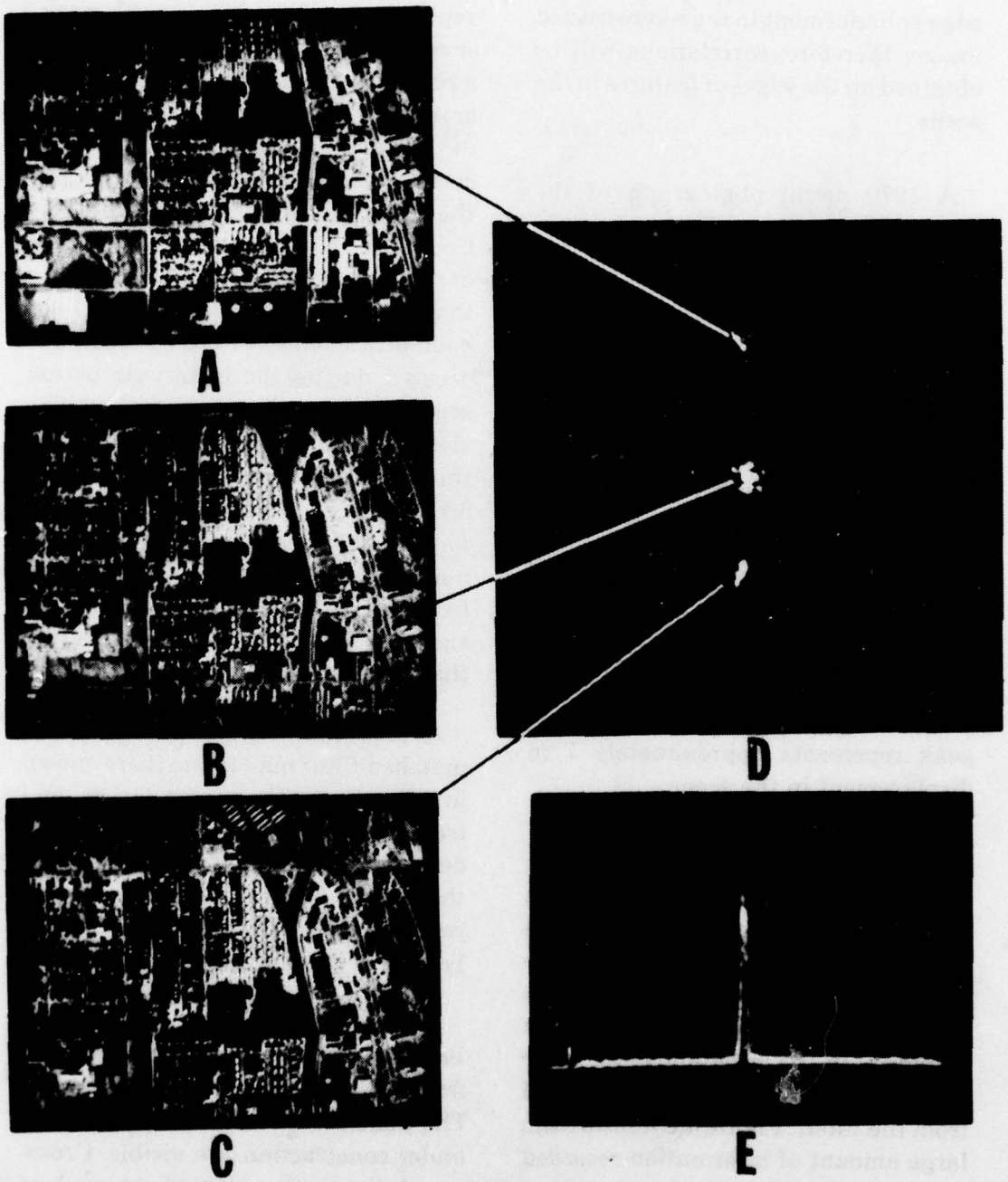


**Figure 3. Correlations using urban scene. (a,b,c) positions of 1970 urban image corresponding to (d) peaks in correlation plane, (e) oscilloscope display of TV line scan through the central cross-correlation peak.**

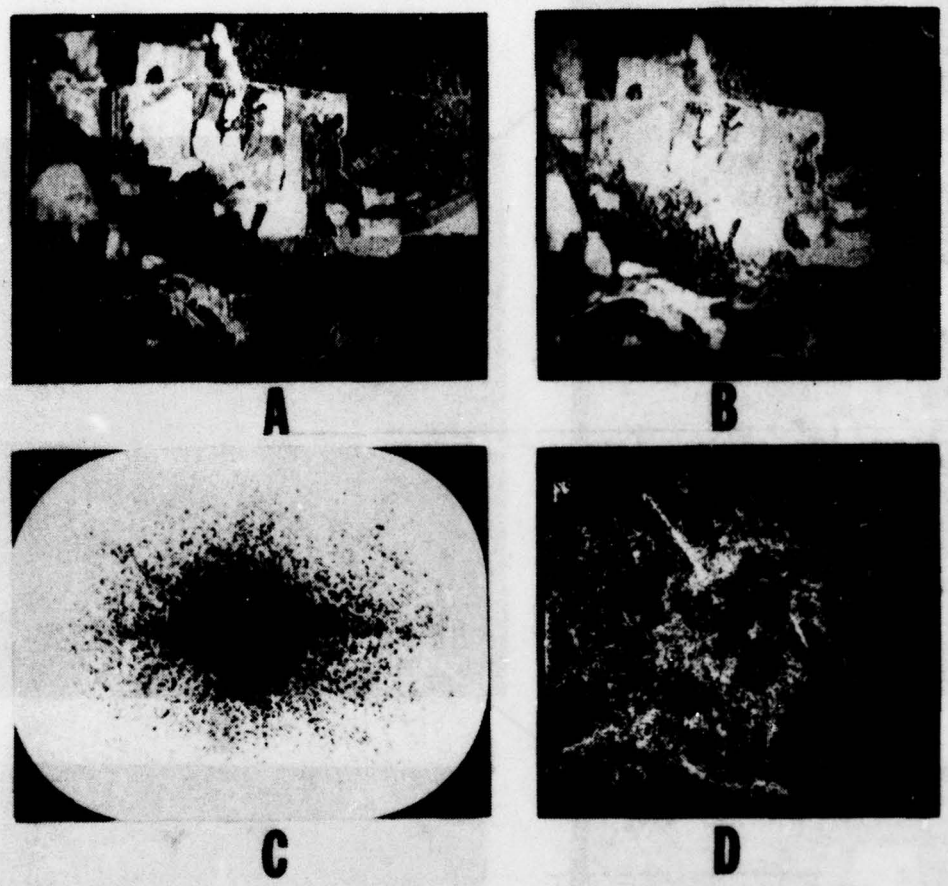


**Figure 4. Rural scene. (a) TV image of rural scene in 1962, (b) modulator output (c) matched filter made from this scene, and (d) image reconstructed from filter.**

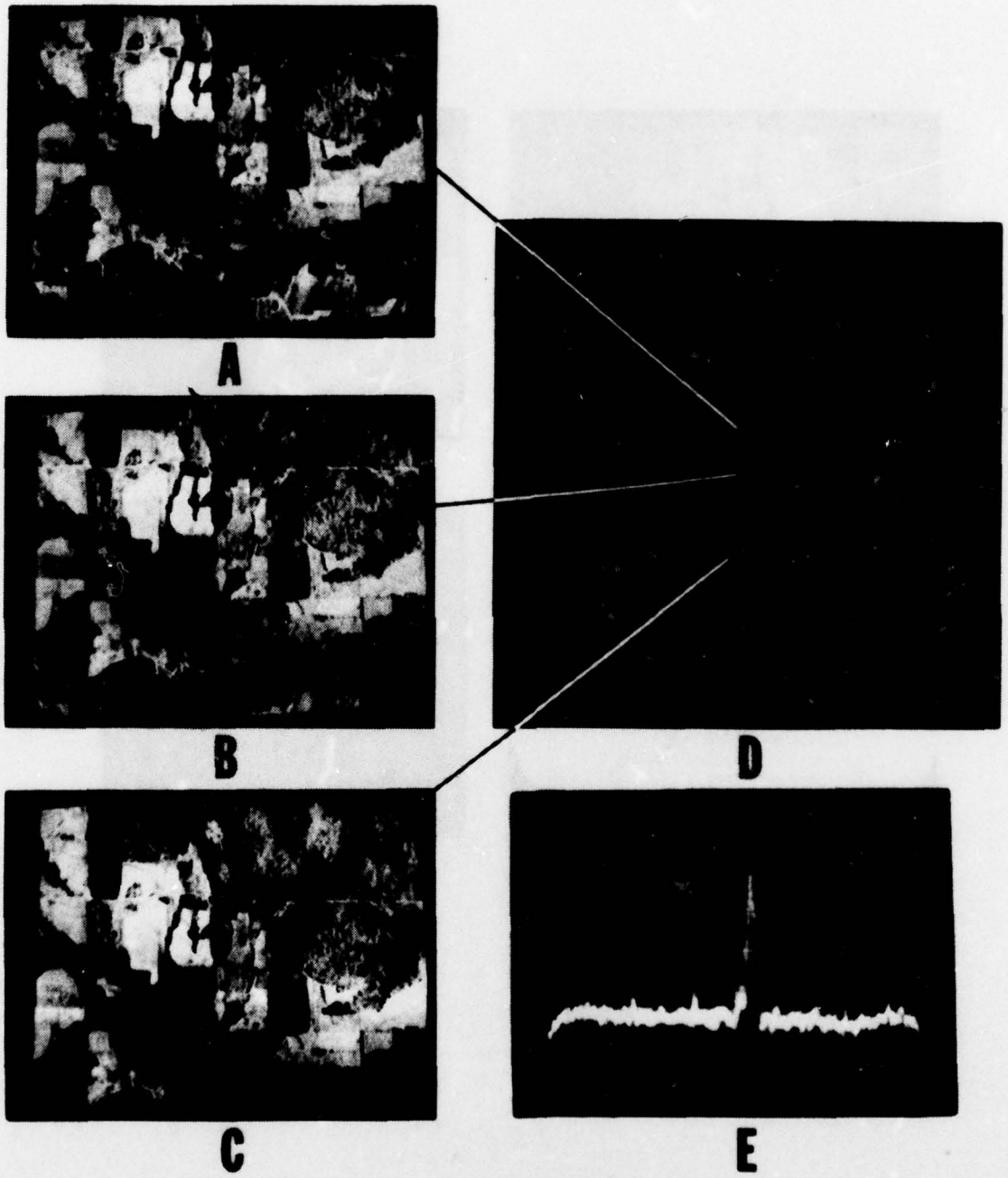


**Figure 5. Correlation using rural scene. (a,b,c) positions of 1970 rural image corresponding to, (d) peaks in correlation plane, (e) oscilloscope display of TV scan through the central cross-correlation peak.**

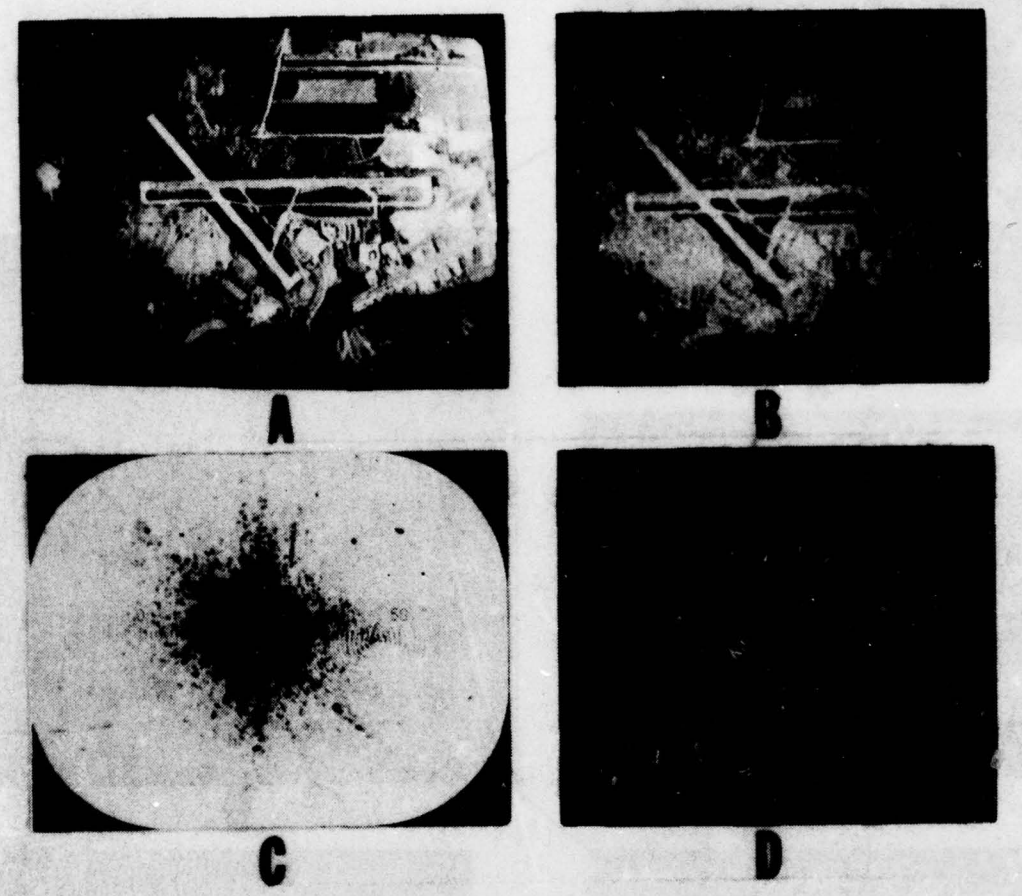


**Figure 6. Airport scene. (a) TV image of airport in 1962, (b) modulator output (c) matched filter made from this scene, and (d) image reconstructed from filter.**

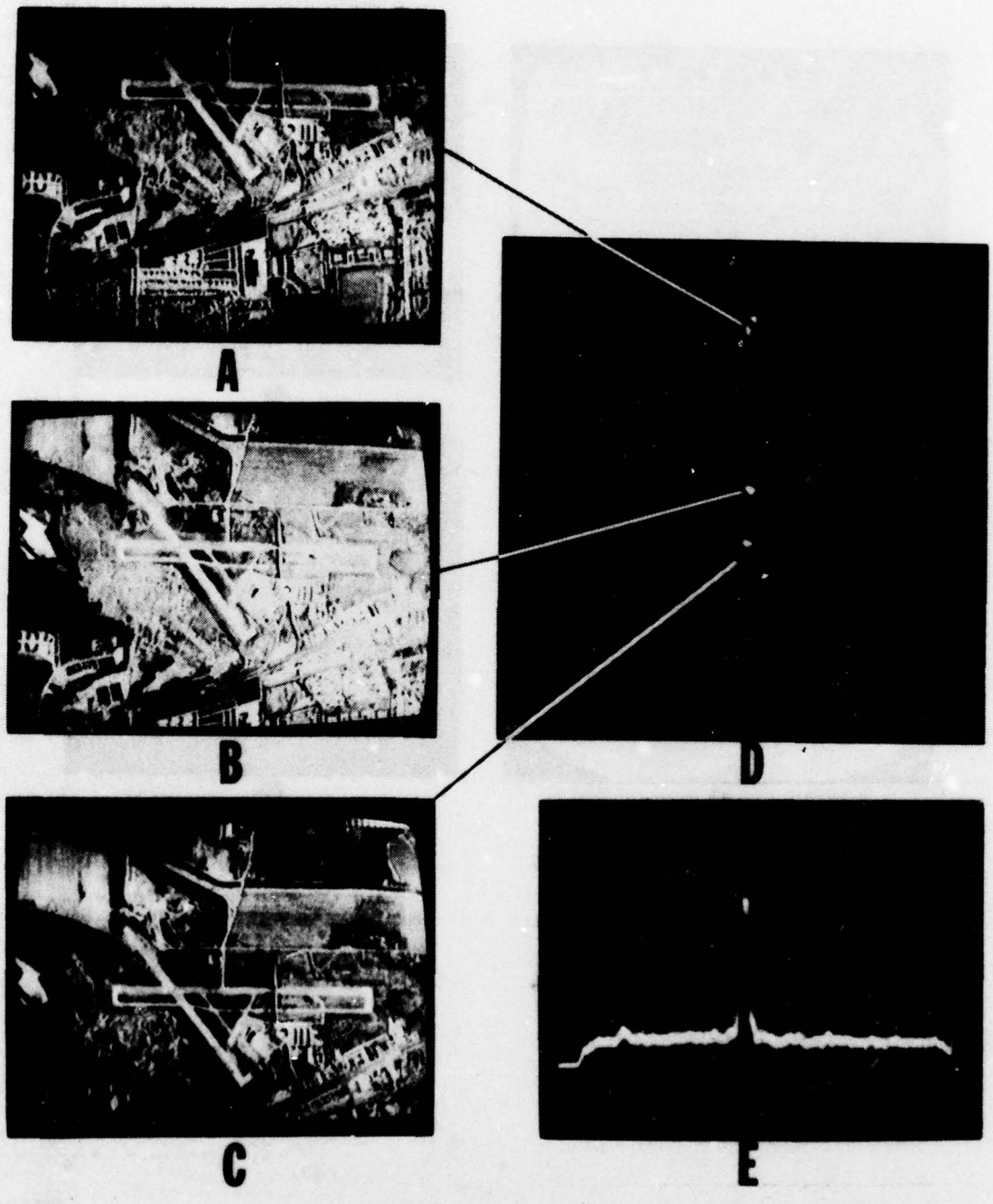


**Figure 7. Correlations using airport scene. (a,b,c) positions of 1970 airport image corresponding to, (d) peaks in correlation plane, (e) oscilloscope display of TV line scan through the central cross-correlation peak.**

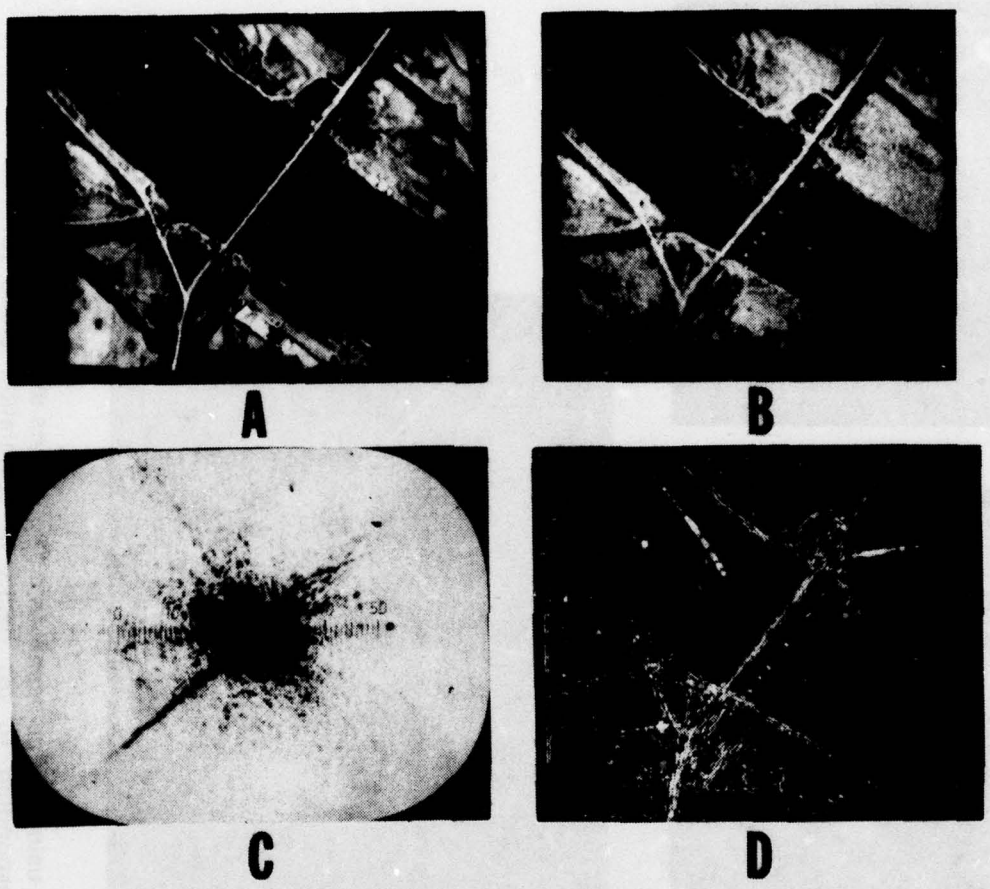


**Figure 8. Bridge scene. (a) TV image of bridges in 1962, (b) modulator output, (c) matched filter made from this scene, and (d) image reconstructed from filter.**

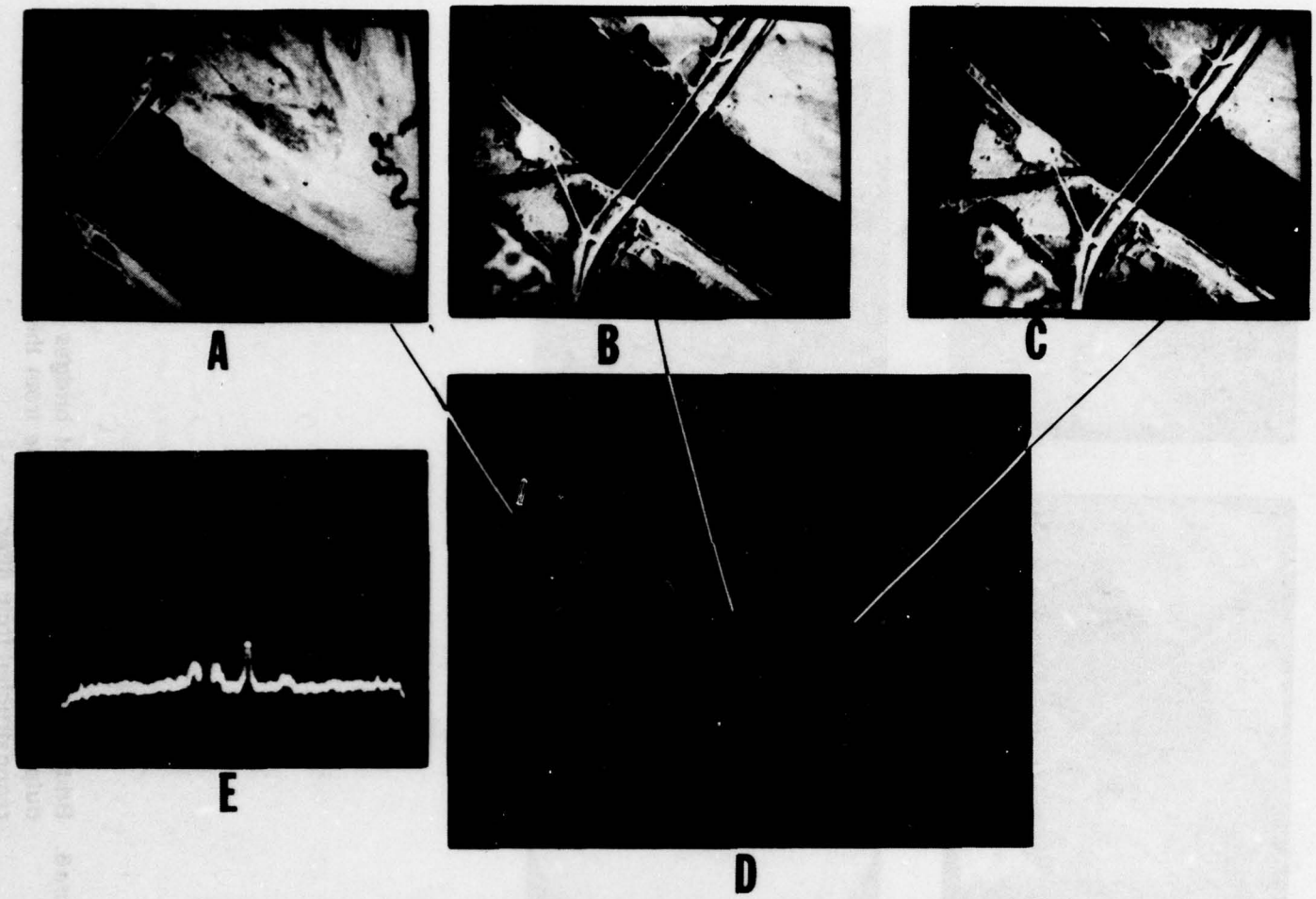


**Figure 9.** **Correlations using bridge scene. (a,b,c) positions of 1970 bridge image corresponding to (d) peaks in correlation plane (e) oscilloscope display of TV line scan through the central cross-correlation peak.**

old bridge and the new bridge in the 1970 view, producing two correlation spots for each position of the 1970 scene. The dominant contribution of the bridges to the correlation spot is illustrated in Figure 10 in which all of the input image except for the bridges was covered by a mask. A strong correlation was still obtained. The correlation for each bridge is a pair of spots, or lines, corresponding to the sides of the bridges.

Some pecularities of correlation on simple linear objects are illustrated in Figures (9) and (10). The bridges and highway approaches are similar over the entire length, therefore, a cross-correlation is obtained between one part of the bridge or highway and any other part producing an elongated correlation spot. This is characteristic of the correlation process itself and is independent of the method, digital or optical, by which the correlation is performed. Although the input image was moved horizonally in Figure 9, the correlation has both a vertical and a horizontal displacement. This can be attributed to a slight angular distortion in the input TV monitor allowing the bridge to cross-correlate with the bridge approach above it in the image as the scene is displaced.

## 4. EXPERIMENTS WITH RADAR IMAGERY

Tests were performed with imagery used in another terminal guidance program. The purpose of these experiments was to determine if the simulated radar imagery would correlate with actual radar imagery and to obtain performance data on which to base an improved correlator design. The simulated radar imagery is shown in Figure 11(A) as it appeared on the TV monitor input to the correlator.

This photograph shows an area estimated to be 5.2 km in diameter and contains both low-resolution areas such as the wide river behind the dam, and higher resolution structures such as roads and hilly terrain. Figure 11(B) shows the image formed by the liquid crystal cell. A matched filter, Figure 11(C), was constructed for this image with a spatial frequency bandpass selected to suppress the average light level and also to have relative good low-frequency response. The filter performed correlations on feature outlines of Figure 11. The spatial frequency range of this filter, 0.2 to 0.8 $l$/mm, was chosen to match the frequency content of the radar imagery. Figure 12 is an enlargement of this filter. The image reconstructed from the filter is shown in Figure 11(C). Its low quality is due in part to problems of extraneous scattered light and low light level.

An actual radar image that was not grossly distorted relative to the simulated image could not be obtained. A scheduling problem prevented the recording of high quality images. The remaining tests were performed with

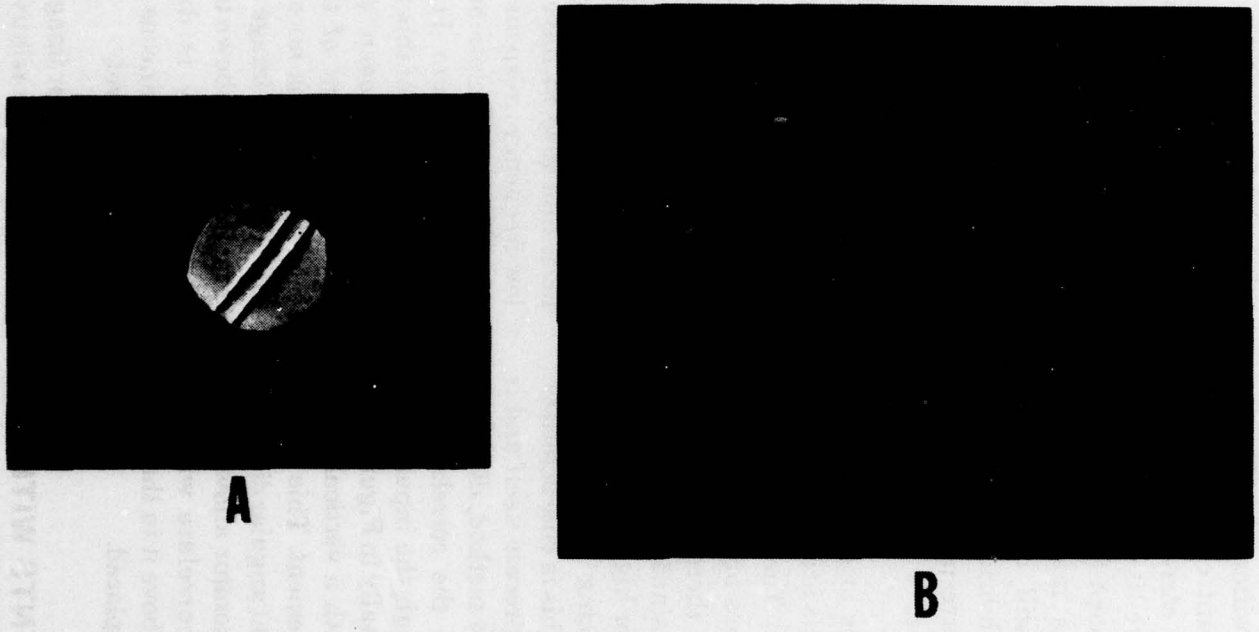


**Figure 10. Correlation of bridge image with bridge scene. (a) TV image of masked 1970 bridge scene and (b) resulting cross-correlation peak.**

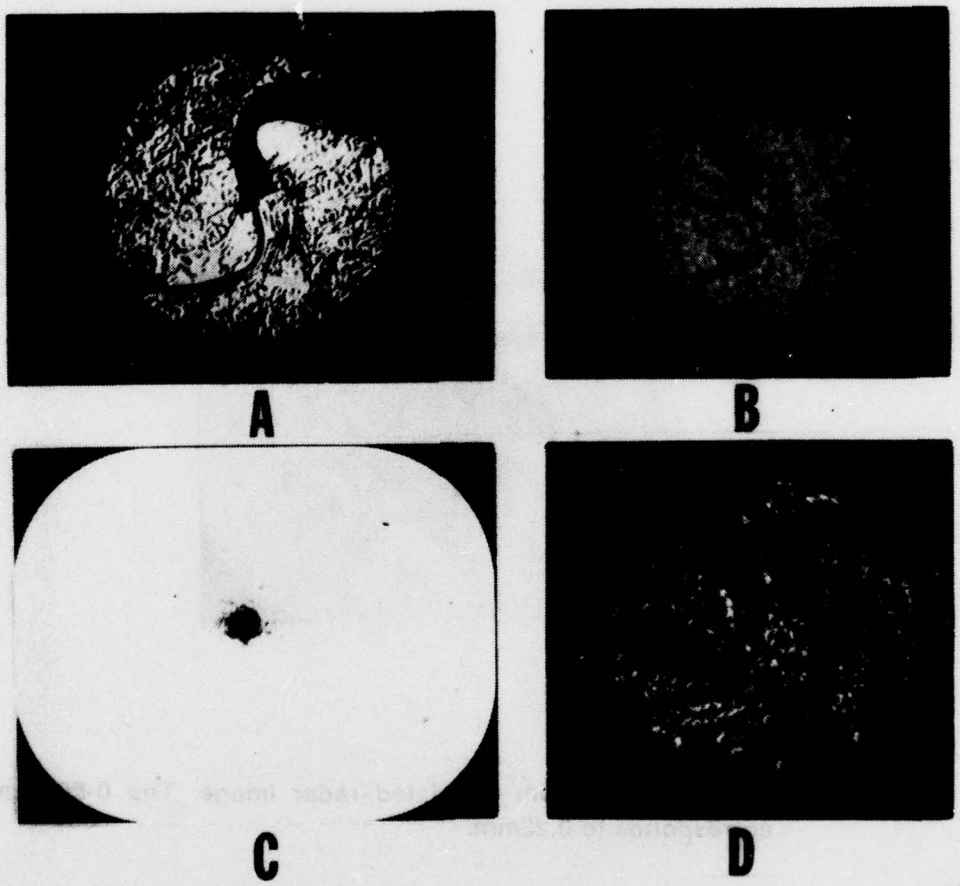


**Figure 11. Simulated radar scene. (a) TV display of simulated radar image, (b) modulator output image, (c) matched filter, and (d) image reconstructed from matched filter.**

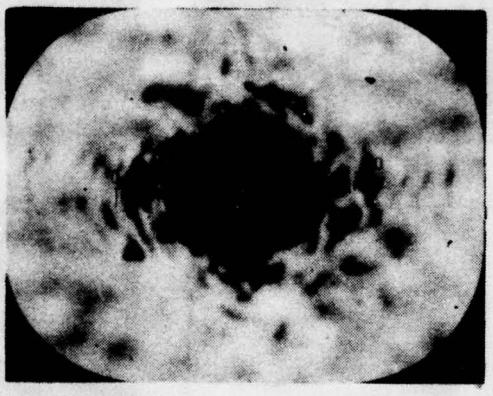

**Figure 12. Matched filter from simulated radar image. The 0-50 scale corresponds to 0.22mm.**

the original simulated radar image and therefore were auto-correlations. Figure 13(A) shows the correlation plane and 13(B) is a trace through the center of the auto-correlation peak as detected by the TV camera at the output of the correlator. The correlation is distinct and well above noise level. The half-power width is 1/60 of the width of the input image. Since the image was displayed on one-half the TV monitor screen, it was estimated that the image resolution was approximately 130 pixels across. It should be possible to estimate the center of this peak to at least 1/5 of its width, thus giving an estimated accuracy of 1/300 or 0.3% of image width. This appears to be more than adequate accuracy, especially in view of the probable errors between simulated and real radar imagery.

The required filter alignment and input scale and rotational alignment accuracies were determined by adjusting the system until 50% decrease in the height of the correlation peak was observed. The results are listed in Table 1.

To test the possibility of detecting correlation peaks with a Reticon detector array, the TV camera was replaced with a linear Reticon array. A short focal length lens was used to focus the correlation peak on one cell. Figure 14 shows the correlation peak detected with the Reticon. The length of the trace corresponds to 6.8 mm.

A measurement was made of the light energy incident on the input image and the energy in the correlation peak. Energy input over the 12.5 mm diameter image was 1.5mW and the energy in the correlation peak was $5 \times 10^{-3}\mu W$ or -55 dB. No attempt was made to improve or optimize the system efficiency.

In an operational terminal guidance correlator it would probably be necessary to generate the filter on a separate optical system and load it into the correlator. A matched filter was recorded using one liquid crystal modulator and the correlation was performed in the same system using a different modulator. The correlation spot amplitude and signal-to-noise ratio were the same as those measured using one modulator to both record the filter and to input the image to be correlated. Therefore, for this application the modulators are interchangeable and the differences in response and uniformity have no significant effect.

Several problems were observed with the present system. One was an erratic correlation peak height fluctuation possibly caused by voltage instabilities in the video components. Another was the TV monitor picture size change as a function of average image size and brightness setting. As a result, when part of the image was blocked to determine the change in correlation peak with the input image

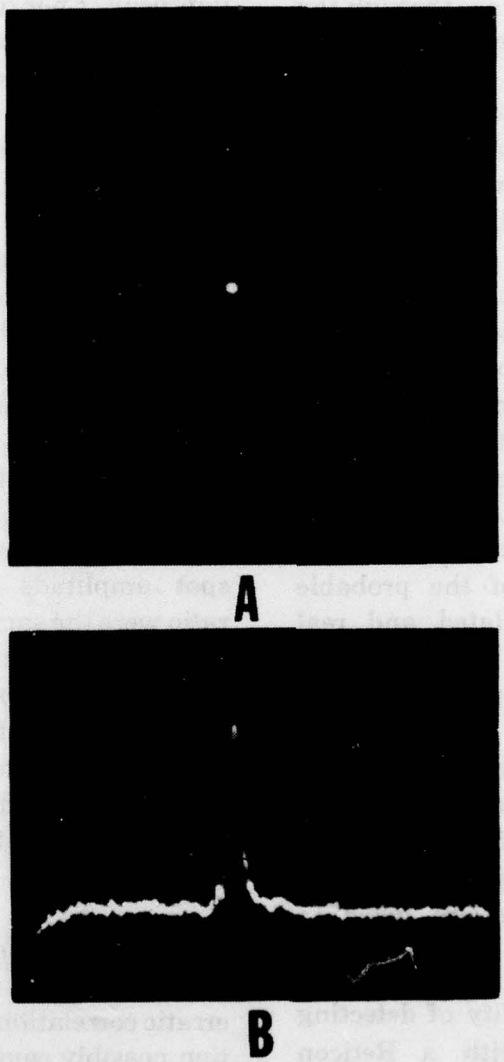


**Figure 13. Auto-correlation of simulated radar scene. (a) correlation plane and (b) oscilloscope display of TV line scan through the image auto-correlation peak.**

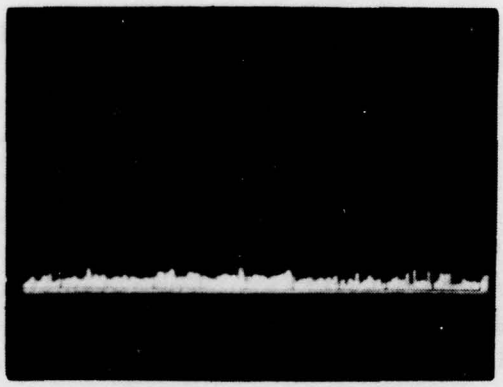

**Figure 14. Auto-correlation peak detected by Reticon photodiode array.**

**Table 1. Matched Filter Alignment Tolerances**

| Parameter | Required Alignment Accuracy | Total Misalignment Tolerance |
|---|---|---|
| Lateral filter position | ±12 $\mu$m | 24 $\mu$m |
| Image and filter rotation | ±2° | 4° |
| Image Scale | ±4.3% | 8.6% |

area displayed, the effect due to scale change was much greater. These difficulties can be solved by using a higher quality TV camera and monitor.

## 5. PROPOSED CORRELATOR CONFIGURATION AND PERFORMANCE ESTIMATES

### A. Image and Filter Format

The requirements for an optical correlator for an all weather terminal guidance application will be discussed in this section. Desirable features of a correlator are low cost, compactness, lightweight, low power consumption, ruggedness and reliability, large data handling capacity, and high speed. Correlator configurations are dependent upon the input image size and resolution. It will be assumed that this correlator is to operate on low-resolution images with relatively few pixels. As the input data, the image will be assumed to consist of 128 × 128 or $1.64 \times 10^4$ pixels and the reference image from which the matched filter is made to consist of 256 × 256 or $6.55 \times 10^4$ pixels. It is desirable to have the reference image larger than the input scene, because lateral displacement between the input and reference images can occur. Having the reference larger than the input insures that the correlation peak amplitude will not vary due to relative lateral displacement of the images.

For a reasonable balance between input image size and its Fourier transform size, we shall choose an input image format of 22 pixels/mm which gives an image size of 6 × 6 mm, and a reference image twice as large, or 12 × 12 mm in size will be chosen. If the Fourier transform lens has a 200 mm focal length and laser diodes are used as light sources with $\lambda$=820 nm, the maximum diameter of the Fourier transform is ±1.8 mm for data and ±3.6 mm for sampling frequency. For a correlation peak displayed at a distance of 200 mm from the Fourier transform plane, the minimum size of the correlation spot should be approximately 200 $\mu$m. The location of this spot should be within an area of 6 × 6

mm in size if the input image is to overlap the reference completely. A detector having a resolution of 100$\mu$m should be sufficient and the area covered need not exceed 6 × 6 mm. While the half-power width of the peak should be 100$\mu$m or more, for more precise estimation of the location of the peak, finer detector resolution should be used. As a minimum, 100 $\mu$m detector resolution is needed to detect correlation peaks while 20 $\mu$m resolution would provide a much better estimate of the location of the correlation peak, to approximately 1/5 the width of the correlation peak.

The input image may not have the correct scale, angular orientation or aspect angle as compared to the reference image. Therefore, it is desirable for an optical correlator to perform scale, angular orientation, and possibly aspect angle searches. Furthermore, correlations are required for different input images as the missile closes with the target. To perform these operations in a reasonable time and with minimum complexity, it is desirable to perform as many correlations as possible without requiring a change of the matched filter assembly.

Using a cathode ray tube (CRT) or an equivalent input device as in Figure (1), scale search can be performed by changing the CRT deflection amplifier gain to change the image size. For example, image size could be changed in ten 5% steps from 75% to 120% of the nominal image size. This search could be performed electronically and at the scan rates of the display. By changing the horizontal gain as a function of vertical position small aspect angle changes (distortions) can be searched.

### B. Filter Multiplexing

Multiplexing can be performed by the use of several input image illuminating beams and numerous parallel filters at the Fourier transform plane. Figure 15 shows the basic arrangement. At the left are several light sources which can be turned on either one at a time or simultaneously. These sources might be laser diodes, for example. Light from each source passes through the input image and forms a Fourier transform that is separate from those of adjacent light sources. A different matched filter can be located at each transform location. The correlation from each source can be made to coincide at the output plane or appear at separate locations. If the correlations appear at separate locations at the output plane, then each correlation would have its own detector and the correlations could be performed simultaneously; the latter arrangement is faster but requires multiple detector arrays. All of the light from each source is used to perform correlations with one filter. To keep the complexity to a reasonable level, an array of up to 5 × 5 light sources for a total of 25 parallel processors could be used.

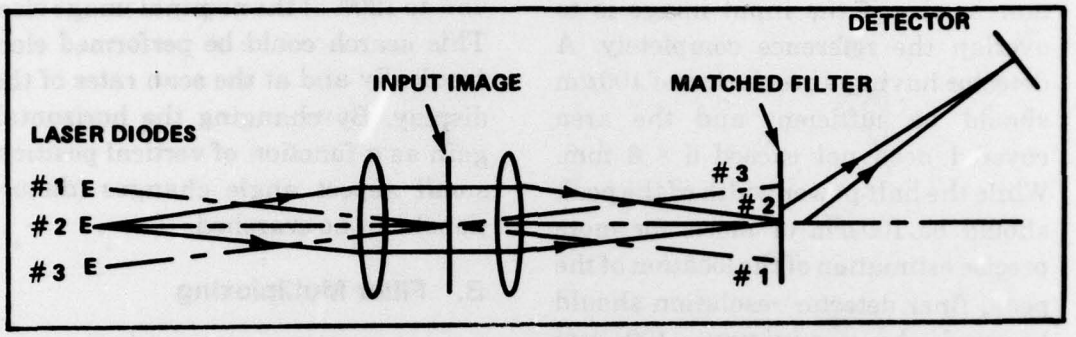


**Figure 15. Matched filter multiplexing with multiple light sources.**

Another method of multiplexing was described by Vander Lugt [7]. Numerous filters are superimposed at the same location in the Fourier transform plane so that correlation peaks from each are located separately at the output, as shown in Figure 16. This arrangement requires multiple detectors in the output plane. The number of such superpositions is limited by space available at the output plane and by the fact that light is equally divided between all correlations and thus, decreases as 1/N, where N is the number of superimposed filters. Vander Lugt demonstrated the use of nine superimposed filters which seems to be a realistic maximum number.

Using both multiplexing techniques simultaneously, a total of 9 × 25 or 225 different filters could be recorded at the Fourier transform plane. If the scale search for 10 different image sizes for each of the 225 filters is included, this correlator could perform a total of 2,250 different correlations. These 225 filters might include different images, angular orientations, or aspect angles. If filter assemblies are physically replaced, then the number 225 can be multiplied by the number of such replacements.

### C. Estimate of Correlation Time

An optical correlator takes a Fourier transform and performs correlations almost instantaneously. Time is required to load the image into the correlator and to read out the results. The readout of data is limited by the rate of scanning the output device and by the light energy used in the processor to charge light detector cells. The time to load the image into the processor is determined both by the scan rate of the sensor or sensor display and by the response time of the light modulator.

As an example a Reticon 100 × 100 element detector array will be considered. Several of these detector arrays might be used in parallel to perform parallel correlations. The specifications

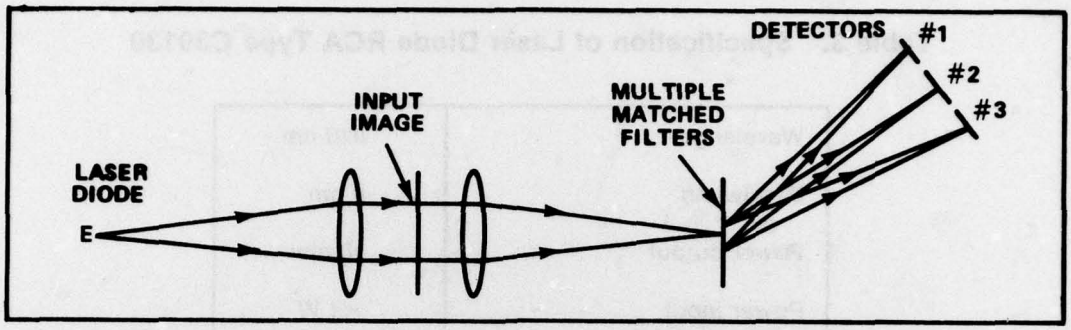


**Figure 16. Matched filter multiplexing with superimposed filters.**

of this detector are listed in Table 2. The maximum scan rate is 10 MHz resulting in one complete output plane scan in 1 millisec. After each scan a different laser diode is turned on and 1 msec is expended to charge the detector for a total of 2 msec for a correlation.

A 10 mw laser diode with output at 820 nm and having 4 nm spectral bandwidth can be used in the correlator. The specifications of a typical diode are listed in Table 3. Its switching time is less than one nanosecond, and therefore, can be considered instantaneous. Its wavelength matches the peak response of the detector array. It is estimated that approximately 10% of its output energy will enter the correlator. As many as 25 diodes can be used to illuminate the correlator, one diode at a time.

**Table 2. Reticon Detector Array RA 100 × 100**

| | |
|---|---|
| Detector array | 100 × 100 elements, $10^4$ pts |
| Element spacing, center to center | 60 $\mu$m |
| Active area | 6 × 6 mm |
| Saturation exposure | 8 ergs/cm$^2$ |
| Minimum effective exposure | 0.16 ergs/cm$^2$ |
| Maximum readout rate | 10 MHz ($10^3$ frames/sec) |
| Minimum readout rate | 100 KHz (10 frames/sec) |
| Power consumption of typical complete video camera | 10 W |

**Table 3. Specification of Laser Diode RCA Type C30130**

| | |
|---|---|
| Wavelength | 820 nm |
| Bandwidth | 4 nm |
| Power output | 10 mw |
| Power input | <1 W |
| Emitter area | 2 × 13 m |
| Diode diameter | 10 mm |
| Rise time of emitted pulse | <1 nsec |

The performance data for several input devices are listed in Table 4. Because previously described experiments were performed with the Hughes Aircraft noncoherent-to-coherent image converter and complete specifications are available, the computational estimates used here will be based on this device with a CRT as the source of the image and a lens to image the CRT picture onto the image converter. This arrangement would not be optimum if the signal is in electronic form and direct electronic to coherent optical transducers are becoming available which will result in much more compact systems. Several other transducer specifications are listed in Table 4 describing the Hughes liquid crystal TV display, the Hitachi liquid crystal display, and the photoconductor thermoplastic transducer.

The estimates here are based on the data of the Hughes Aircraft noncoherent-to-coherent image converter. In generation of the input image, it will be assumed that the image data are collected and stored in a digital memory and read onto a CRT which is imaged on the liquid crystal cell. Thus, for a 128 × 128 point array there are 1.6 × $10^4$ points. These can be scanned at a 1.6 MHz rate so that the image is read onto the CRT in 10 msec. Because the crystal response time is 15 msec and turn-off time is 25 msec, it will be assumed that a usable image exists during a 10 msec period from 20 to 30 msec after the start of the scan, and that an additional 20 msec are needed for a complete image turn-off. During these 10 msec, five sequential sets of correlations, each with nine parallel correlations, can be performed for a

## Table 4. Correlator Input Transducers

| Hughes Aircraft Liquid Crystal Noncoherent to Coherent Image Converter | |
|---|---|
| Mode of operation | modulates reflected light |
| Size of active area | 25 × 25 mm |
| Resolution at 50% MTF | 60 lines/mm |
| Maximum number of points | $9 \times 10^6$ |
| Turn-on time | 15 msec |
| Turn-off time | 25 msec |
| Total time per image | 40 msec (25 images/sec) |
| Estimated exposure per image | 15 ergs/cm² |
| Irradiance for full contrast | 100 μw/cm² |
| Light utilization | 25% |
| Drive power | 100 mw estimated |
| Image persistancy | < 25 msec |
| Maximum drive voltage | < 25 V |
| **Hughes Aircraft Liquid Crystal TV Display** | |
| Mode of operation | modulates reflected light |
| Size of active area | 45 × 45 mm |
| Number of points | 175 × 175 ($3 \times 10^4$) |
| Resolution | 4 pts/mm |
| Turn-on time | unknown |
| Turn-off time | unknown |
| Total time per image | estimated at 40 msec |
| Light utilization | 25% |
| Drive power | < 100 mw estimated |
| Image persistancy | < 25 msec estimated |
| Maximum drive voltage | < 25 V |

**Table 4. (Continued)**

| Photoconductor-Thermoplastic Noncoherent to Coherent Image Converter | |
|---|---|
| Mode of operation | transmission, diffraction of image on a carrier frequency |
| Size of active area | 25 × 25 mm |
| Resolution | > 800 lines/mm (carrier frequency) |
| Number of points at 50 pts/mm carrier | $1.5 \times 10^6$ |
| Turn-on time | < 10 msec |
| Turn-off time | ≃ 240 msec |
| Total time per image | 250 msec |
| Exposure per image | 20 ergs/cm² |
| Light utilization | 30% |
| Drive power/image | ≃ 60 ergs/cm² |
| Image persistency | permanent until erased |
| Maximum voltage used in device | 1000 volts |
| **Hitachi Liquid Crystal TV Display** | |
| Mode of operation | modulates transmitted light |
| Size of active area | 120 × 90 mm |
| Number of points | 82 × 109 ($8.9 \times 10^3$) |
| Resolution | 1.1 pts/mm |
| Turn-on time | unknown |
| Turn-off time | unknown |
| total time per image | 200 msec (estimated) |
| Light utilization | 100% |
| Drive power | 10 mw |
| Image persistency | < 200 msec |
| Maximum drive voltage | 15 V |

total of 45 correlations. Thus, in 50 msec, 45 correlations can be performed at an average rate of 900 correlations/sec or 450 correlations in 0.5 sec. If more than 45 correlations need to be performed with each input image, the input image can be continuously rescanned.

The data arrangement for the correlator would depend upon factors such as the angular search or scale search required, the storage of multiple targets, and the total operating time for the correlator. If angle and scale variations are stored as separate filters all 225 filters can be accessed in 250 msec. Scale searches performed by changing the input image size would require re-entering the image scan for each increment. To search 10 scale increments each correlated with up to 45 different filters would require 50 msec for each increment. In another arrangement only 9 of the parallel filters are correlated against 10 scale increments for 25 different images. Table 5 summarizes the performance capability of the correlator for a few examples of input and filter combinations.

**Table 5. Summary of Specifications for Proposed Optical Correlator**

| | | |
|---|---|---|
| Reference data format (filters) | : | 256 × 256 pts. |
| Input image format (real time) | : | 128 × 128 pts. |
| Total number of reference filters | : | 225 |
| Maximum number of scale changes | : | 10 |
| Filter format | : | 25 sets of filters in time sequence, 9 filters per set at a time |
| Correlation time | : | 2 msec per set |
| Image enter and erase time | : | 50 msec (includes 10 msec computation time) |
| Correlator power consumption | : | <2 W |
| Correlator size | : | 1500 $cm^3$ (100 $in.^3$ or 0.05 $ft^3$) |
| Correlator weight | : | 5 kg (12 lb) |

**Computational Capability Per Half-Second Period for Various Data Arrangements**

| New Images | Scale Increments Per Image | Filters Accessed | Correlations |
|---|---|---|---|
| 1 | 1 | 225 | 225 |
| 1 | 10 | 45 | 450 |
| 1 | 10 | 9 | 90 |
| 2 | 5 | 45 | 450 |
| 5 | 1 | 90 | 450 |

Since the laser diodes require 1 W of power and the liquid crystal input device and detector array a fraction of a watt, the total power consumption should be less than 2 W. This does not include the power requirements of the CRT and computer components expected to be used with the correlator. The CRT is not a necessary component as a Hughes Aircraft liquid crystal TV display device could replace the CRT. The charge-coupled-device (CCD) addressed liquid crystal modulator under development by Hughes could be used directly in place of the incoherent to coherent image converter [8]. With the latter arrangement, the computer could be packaged in 1500 $cm^3$ (0.05 $ft^3$) volume and would probably weigh less than 5 kg (11 lb).

## 6. BRASS-BOARD CORRELATOR

Figure (17) shows a proposed design for a correlator to demonstrate the concepts discussed in the previous section. Current state-of-the-art components, listed in Table 6, are used. While the general arrangement is the same as that discussed in the previous sections, this correlator has four superimposed filters instead of nine. This change was considered necessary to reduce complexity and to increase light level in each correlation peak. The image input device is a Hughes Aircraft liquid crystal TV display having 4 pixel/mm resolution. This low resolution makes the input light modulator approximately 33 × 33 mm in size and gives a very small Fourier

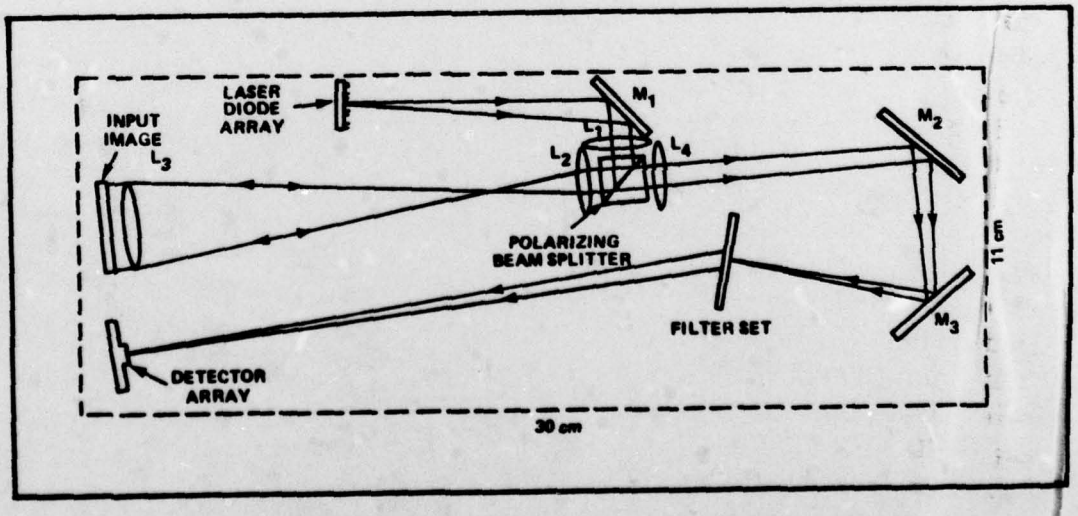


**Figure 17. Brass-board Optical Correlator.**

**Table 6. Brass-Board Correlator Components**

| Lenses | Focal Length | Diameter |
|---|---|---|
| $L_1$ | 100 mm | 20 mm |
| $L_2$ | 25 mm | 12.5 mm |
| $L_3$ | 125 mm | 50 mm |
| $L_4$ | 200 mm | 20 mm |
| Fourier Transform Focal Length | 200 mm | — |
| Light sources: | Laser Diodes, RCA type C 30130 | |
| Detector array: | Reticon RA 100 × 100 | |
| Input light modulator: | Hughes Aircraft Liquid Crystal Display | |

transform. To increase its size the Fourier transform is magnified by lenses $L_2$ and $L_4$ by the ratio of $f_4/f_2$, where f is the lens focal length. The use of the combination $L_2$, $L_3$ allows for the use of a small polarizing beam-splitter and reduces the overall correlator size. The lens combination $L_2$ and $L_3$ also reduces the image size to 6 × 6 mm to the right of lens $L_2$. The preceding lens focal lengths were chosen primarily to achieve a convenient scale and do not represent the minimum possible. For example, others have chosen the focal length of $L_4$ as 100 mm [9]. Overall correlator length can also be reduced by using a smaller input image or by changing the ratio of focal lengths of the combination $L_2$ and $L_3$. For example, if $f_3$ = 125 mm and $f_2$ = 12.5 mm instead of 25 mm, the input image size to the right of $L_2$ would be 3 × 3 mm which would give the same Fourier transform size as above with a shorter focal length, $f_4$ = 100 mm, for $L_4$. The limiting factors in size reduction are lens aberrations, the F-numbers of lenses $L_2$ and $L_4$, and the increasing angular spread of incident rays on the Fourier transform plane. Determining these parameters requires the production of specific lenses and analysis of their aberrations, a task that is beyond the scope of this effort.

The matched filter consists of an array of 5 × 5 filters each occupying 7.2 mm × 7.2 mm of space. At each filter location four different filters are superimposed. The correlation peaks from each fall on a detector array

which could be a Reticon RA 100 × 100 element array. The specifications of this detector are listed in Table 2. One-fourth of this detector could be allocated for each filter giving 50 × 50 elements for each correlation. For the parameters shown in Table 6 the width of the correlation peak can be expected to be approximately 100 $\mu$m while the detector elements are on 60 $\mu$m centers. This allows for some improvement in estimating the location of the peak. Choosing a different filter-to-detector distance and possibly using a larger detector array would allow for more precise location of the correlation peak.

The Reticon RA 100 × 100 detector consists of 10,000 photodiodes arranged in a 100 × 100 matrix on a single silicon chip. Each diode has a capacitance and a MOS multiplex switch. The chip has a MOS shift register for scanning. Readout is obtained by discharging the capacitors of the diodes in sequence through a video line, causing a current in the line in proportion to the photocurrent in the diode integrated over the scan time. This arrangement gives the diode an effective sensitivity $10^4$ times that of a similar diode array operated in the photoconductive mode. Scan speed can be traded directly for sensitivity because as the scan rate decreases, sensitivity increases. The peak of the spectral sensitivity curve matches that of the laser diode output at 820 $\mu$m.

The laser diode characteristics are listed in Table 3. Of the 10 mW output approximately 10% can be expected to be utilized which should give sufficient light output at the detector array. It has low power consumption and fast switching speed.

The matched filter array would be constructed on an optical system separate from the correlator. The filters could either be recorded on a high resolution photographic emulsion, on dielectric materials such as dichromated gelatin for higher efficiency, or on thermoplastic photoconductive recording materials. The latter would be most suitable for operational systems because it is nearly real time and the recording is permanent until erased.

## REFERENCES


1. Clary, J. B., *All-Digital Correlation for Missile Guidance* Final Report for Battelle Task D. O. No. 0144, 17 December 1976.

2. Guenther, B. D., Christensen, C. R. Greer, M. O., and Rotz, F. B. *Optical Cross Correlation for Terminal Guidance,* Proceedings of the AIAA Guidance and Control Conference, Stanford, CA, 14-16 August 1972.

3. Preston, K., Jr., *A Comparison of Analog and Digital Techniques for Pattern Recognition,* Proc IEEE, Volume 60, 1972, p. 1216.

4. Shareck, M. W., and Castle, J. G., Jr., *Area Correlation by Fourier Transform Holography.* Final Report, USA MICOM contract DAAHO1-72-C-0916, the University of Alabama in Huntsville, November 1973.

5. Grinberg, J., Jacobson, A. J., Bleha, W., Miller, L., Fraas, L., Boswell, D., Myer, G., *A New Real-Time Non-Coherent to Coherent Light Image Converter, The Hybrid Field Effect Liquid Crystal Light Valve,* Opt. Eng., Volume 14, 1975, p. 217.

6. Gara, A. D., *Real-Time Optical Correlation of 3-D Scenes,* Appl, Opt., Volume 16, 1977, p. 149.

7. Vander Lugt, A. and Leith, E. N., *Techniques in Optical Data Processing and Coherent Optics,* Ann. N. Y. Acad. Sci., Volume 157, 1969, p. 99.

8. Grinberg, J., Bleha, W. P., Braatz, P. O., Chow, K., Close, D. H., Jacobson, A. D., Little, M. J., Massetti, N., Murphy, R. J., Nash, J. G., and Waldner, M., *Liquid-Crystal Electro-Optical Modulators for Optical Processing of Two-Dimensional Data,* Proceedings SPIE, Volume 128, 1977, p. 253.

9. Fienup, J. R., Colburn, W. S., Chang, B. J., and Leonard, C. D., *Compact Real-Time Matched Filter Optical Processor,* Proceedings SPIE, Volume 118-04, 1977

# DISTRIBUTION

No. of Copies

Commander
Defense Documentation Center
Attn: DDC-TCA 2
Cameron Station
Alexandria, VA 22314

Commander
US Army Research Office
Attn: Dr. R. Lontz 2
P. O. Box 12211
Research Triangle Park,
NC 27709

US Army Research and Standardization Group (Europe)
Attn: DRXSN-E-RX, Dr. Alfred K. Nedoluha 2
Box 65
FPO, New York 09510

US Army Material Development and Readiness Command
Attn: Dr. Gordon Bushy 1
Dr. James Bender 1
Dr. Edward Sedlak 1
5001 Eisenhower Avenue
Alexandria, VA 22333

Headquarters
Hq
DA (DAMA-ARZ) 2
Washington, D. C. 20301

Director of Defense Research and Engineering
Engineering Technology
Attn: Mr. L. Weisberg 2
Washington, D. C. 20301

Director
Defense Advanced Research Project Agency/STO
Attn: Maj. J. T. Karem, Jr. 1
Commander T. F. Wiener 1
D. W. Walsh 1
1400 Wilson Boulevard
Arlington, VA 22209

Commander
US Army Aviation Systems Command 1
12th and Spruce Streets
St. Louis, MO 63166

Director
US Army Air Mobility Research and Development Laboratory 1
Ames Research Center
Moffett Field, CA 94035

Commander
US Army Electronics Command
Attn: DRSEL-TL-T, Dr. Jacobs 1
DRSEL-CT, Dr. R. Buser 1
DELEW-E, Henry E. Sonntag 1
Fort Monmouth, NJ 07703

Director
US Army Night Vision Laboratory
Attn: John Johnson 1
Fort Belvoir, VA 22060

Commander
US Army Picatinny Arsenal 1
Dover, NJ 07801

Commander
US Army Harry Diamond Laboratories
2800 Powder Mill Road 1
Adelphi, MD 20783

Commander
US Army Foreign Science and Technology Center
Attn: W. S. Alcott 1
Federal Office Building
220 7th Street, NE
Charlottesville, VA 22901

Commander
US Army Training and Doctrine Command 1
Fort Monroe, VA 22351

Director
Ballistic Missile Defense Advanced Technology Center
Attn: ATC-D, R. E. Dace 1
J. M. McKay 1
ATC-O 1
ATC-R, B. Vatz 1
ATC-T 1
P. O. Box 1500
Huntsville, AL 35808

Commander
US Naval Air Systems Command
Missile Guidance and Control Branch 1
Washington, D.C. 20360

Chief of Naval Research Department of the Navy
Washington, D.C. 1
Commander
US Naval Air Development Center
Warminster, PA 18974 1

Commander
US Naval Electronics Lab Center
San Diego, CA 92152 1

Director
Naval Research Laboratory
Attn: Dave Ringwolt 1
Code 5570, T. Gialborinzi 1
Washington, D. C. 20390

Commander
Rome Air Development Center
US Air Force
Attn: James Wasielewski, IRRC 1
Griffiss Air Force Base, NY 13440

Commander
US Air Force, AFOSR/NE
Attn: Dr. J. A. Neff 1
Building 410
Bolling Air Force Base
Washington, D. C. 20332

Commander
US Air Force Avionics Laboratory
Attn: D. Rees 1
W. Schoonover 1
Dr. E. Champaign 1
Dr. J. Ryles 1
Gale Urban 1
David L. Flannery 1
Wright Patterson Air Force Base, OH 45433

Commander
AFATL/LMT, Charles Warren 1
Eglin Air Force Base, FL 32544

Environmental Research Institute of Michigan
Radar and Optics Division
Attn: Dr. A. Kozma 1
Dr. C. C. Aleksoff 1
Juris Upatnieks 1
P. O. Box 618
Ann Arbor, MI 41807

Dr. J. G. Castle
Physics Department
University of Alabama
4701 University Drive, N.W.
Huntsville, AL 35807 1

Science and Technology Division
Institute of Defense Analysis
Attn: Dr. Vincent J. Corcoran 1
400 Army-Navy Drive
Arlington, VA 22202

Optical Science Consultants
Attn: Dr. D. L. Fried 1
P. O. Box 388
Yorba Linda, CA 92686

Commander
Center for Naval Analyses
Attn: Document Control 1
1401 Wilson Boulevard
Arlington, VA 22209

Raytheon Company
Attn: A. V. Jelalian 1
528 Boston Post Road
Sudbury, MA 01776

Dr. J. W. Goodman
Information Systems Laboratory
Department of Electrical Engineering
Stanford University
Stanford, CA 94305 1

Eric G. Johnson, Jr.
National Bureau of Standards
325 S. Broadway
Boulder, CO 80302 1

M. Vanderlind
Battelle Columbus Labs
505 Ring Ave.
Columbus, OH 43201 1

Dr. Nicholas George
The Institute of Optics
University of Rochester
Rochester, NY 14627 1

DRDMI-T, Dr. Kobler 1
James Fagen 1
DRDMI-H, Dr. J. P. Hallowes, Jr. 1
DRCPM-PE 1
DRDMI-NS, Jerry Hagood 2

DRDMI-TE W. Pittman 1
R. Russell 1
C. E. Kulas 1
Lewis G. Minor 1
DRDMI-TG 1
TG James A. McLean 1
TD 1
TB 3
DRDMI-C 1
DRDMI-Y 1
DRDMI-HR, Dr. R. L. Hartman 1
Dr. J. S. Bennett 1
Dr. C. R. Christensen 1
Dr. B. D. Guenther 1
Dr. J. L. Smith 1
Dr. J. D. Stettler 1
DRDMI-HRO 1

DRDMI-HRO 60
DRCPM-PE-E, John Pettitt 1

Naval Avionics Facility
Indianapolis, IN 46218 1

F. B. Rotz
Harris Corp.
P. O. Box 37
Melbourne, FL 32901 1

Robert L. Kurtz
TAI Corp.
8302 Whitesburg Dr., S.E.
Huntsville, AL 35802 1

J. R. Vyce
Itek Corp.
10 Maguire Road
Lexington, MA 02173 1

Dr. David Cassasent
Carnegie Mellon University
Hamerschage Hall, Rm 106
Pittsburgh, PA 15213 1

David M. Karnes
McDonnell Douglas Astronautics
5301 Boisa Ave.
Huntington Beach, CA 92647 1

Gerald B. Brandt
Westinghouse Electric Corp.
Research and Development Center
Pittsburgh, PA 15235 1

K. G. Leib
Research Department
Grumman Aerospace Corp.
Bethpage, NY 11714 1

Terry Turpin
Dept. of Defense
9800 Savage Road
Ft. George G. Meade, MD 20755 1

Dr. Stuart A. Collins
Electrical Engineering Dept.
Ohio State University
1320 Kennear Rd.
Columbus, OH 43212 1

Mike Scarborough, MS-19
Teledyne Brown Engineering
Cummings Research Park
Huntsville, AL 35807

Commander
AFEL
Hanscom Air Force Base, MD 01731 1

Dr. Donald H. Close 1
Dr. Jan Grinberg 1
Dr. Wilfried O. Eckhardt 1
Hughes Research Laboratories
3011 Malibu Canyon Road
Malibu, CA 90265

Alphonse C. Elser 1
U. S. Army Engineering Topographic Lab.
Ft. Belvoir, VA 22060

H. J. Caulfield 1
Aerodyne Research, Inc.
Bedford Research Park
Crosby Drive
Bedford, MA 01730



☆U.S. GOVERNMENT PRINTING OFFICE 1978—640-122/190 REGION NO. 4